

## Electromagnetic form factors of the SU(3) octet baryons in the semibosonized SU(3) Nambu–Jona-Lasinio model

Hyun-Chul Kim,<sup>\*</sup> Andree Blotz,<sup>†</sup> Maxim V. Polyakov,<sup>‡</sup> and Klaus Goeke<sup>§</sup>

*Institute for Theoretical Physics II, P.O. Box 102148, Ruhr-University Bochum, D-44780 Bochum, Germany*

(Received 25 April 1995)

The electromagnetic form factors of the SU(3) octet baryons are investigated in the semibosonized SU(3) Nambu–Jona-Lasinio model (chiral quark-soliton model). The rotational  $1/N_c$  and strange quark mass corrections in linear order are taken into account. The electromagnetic charge radii of the nucleon and magnetic moments are also evaluated. It turns out that the model is in remarkably good agreement with the experimental data.

PACS number(s): 13.40.Gp, 13.40.Em, 14.20.Dh, 14.20.Jn

### I. INTRODUCTION

In spite of the belief that quantum chromodynamics (QCD) is the fundamental underlying theory of the strong interaction, low energy phenomena such as static properties of hadrons defy solutions based on QCD. The pertinacity of QCD in the low energy region have led to efforts to construct an effective theory for the strong interaction. In pursuit of this aim, the chiral quark-soliton model, also known as the semibosonized Nambu–Jona-Lasinio (NJL) model, emerged as a successful effective theory to describe the low-energy phenomena without loss of important properties of QCD such as chiral symmetry and its spontaneous breaking.

Originally, the idea of finding the soliton in a model with quarks coupled to pions was realized by Kahana, Ripka, and Soni [1] and Birse and Banerjee [2]. The bound states of the valence quarks were well explored in the model while it suffered from the vacuum instability [3]. This problem of the vacuum instability was solved by Diakonov and Petrov [4]. Having investigated the instanton picture of the QCD vacuum in the low-momenta limit in Ref. [4], they have shown that the low-momenta theory is equivalent to the quark-soliton model free from the vacuum instability. The model was further elaborated in Ref. [5] so that it could predict the static properties of the nucleon in the gradient approximation.

The baryon in this model is regarded as  $N_c$  valence quarks coupled to the polarized Dirac sea bound by a nontrivial chiral field configuration in the Hartree approximation [5–8]. The identification of the baryon quantum numbers is acquired by the semiclassical quantization [5,9] (in nuclear physics called the cranking method [10]) which is performed by integrating over the zero-mode fluctuations of the pion field around the saddle point. It makes the baryon carry proper quantum numbers like spins and isospins. In SU(2),

the model enables us to describe quantitatively a great deal of static properties of the nucleon such as  $N$ - $\Delta$  splitting [8,11], axial constants [8,12,13], electromagnetic form factors [14,15], and to some extent also magnetic moments [8,15].

Although the SU(2) version of the model was quite successful to explain many static properties of the nucleon, it is necessary to extend the model from SU(2) to SU(3) so that it can be possible to examine the same properties of hyperons and moreover to investigate the effects of hidden strangeness on the nucleon which are, in particular, manifested in the  $\pi N$   $\sigma$  term [16,17], the isosplitting of the baryonic masses [18], and strange form factors [19]. Blotz *et al.* [22,23] and Weigel *et al.* [24] have carried out the extension of the model from SU(2) to SU(3). Starting from the semibosonized NJL-type Lagrangian, they have shown that the model describes hyperon spectra successfully. The extended SU(3) model is distinguished from the SU(2) NJL in two ways: First, the mixed terms of the pure SU(2) part and the strange vacuum part are induced by the trivial embedding of the SU(2) soliton into SU(3). Second, since the mass of the strange vacuum part is not negligible, one has to take into account the mass term in the effective action explicitly. The mass corrections are treated perturbatively in linear order. It was shown that the perturbative treatment of the  $m_s$  in the NJL model describes the octet-decuplet mass splitting [22,23] very well and plays an essential role in the mass splitting of hyperons. These two differences determine the characteristics of the SU(3) NJL model.

References [22,24] indicate that the SU(3) NJL provides a more refined structure of the collective Hamiltonian than that provided by the pseudoscalar Skyrme model. A comparable structure can be obtained in the Skyrme model only by introducing explicit vector mesons. However, it is inevitable to import large numbers of parameters into the Skyrme model with vector meson, while the parameters in the NJL model can be fixed completely by adjusting mesonic masses and decay constants ( $f_\pi, f_K$ ). The only free parameter we have is the constituent quark mass arising as a result of the spontaneously broken chiral symmetry. This parameter is fixed by adjusting the mass splitting [23] properly.

It is of great importance that  $1/N_c$  rotational corrections are taken into account. Starting from the path integral for-

<sup>\*</sup>Electronic address: kim@hadron.tp2.ruhr-uni-bochum.de

<sup>†</sup>Present address: Department of Physics, State University of New York, Stony Brook, New York 11794.

<sup>‡</sup>On leave of absence from Petersburg Nuclear Physics Institute, Gatchina, St. Petersburg 188350, Russia.

<sup>§</sup>Electronic address: goeke@hadron.tp2.ruhr-uni-bochum.de

malism, when we integrate over zero-mode fluctuations around the saddle point, a time-ordered product of collective operators appears. The  $1/N_c$  contribution survives because of the noncommutivity of the collective operators [12]. It was examined in detail in Ref. [13] by calculating the axial vector constants  $g_A$  and isovector magnetic moments in SU(2). In the same spirit, the SU(3) model was applied to obtain the axial constants  $g_A^{(3)}$ ,  $g_A^{(8)}$ , and  $g_A^{(0)}$  [20,21,25–27]. It predicted the experimental data within about 10%.

In a recent paper, we have proceeded to evaluate the magnetic moments [28]. The magnetic moments of the SU(3) octet baryons predicted by the present model are in a remarkable agreement with the experiments.

Now, we are in a position to study the electromagnetic form factors and other form factors such as strange form factors. It is important to investigate the form factors in our model, since it allows us to take a step forward in studying dynamics. Hence, as a first phase, we will consider the electromagnetic form factors. It is of great significance to know them in the SU(3) NJL in that not only they provide us with the electromagnetic informations but also allow us to proceed to explore the techniques for the form factors of the neutral ( $Z^0$ ) currents and charged weak ( $W^\pm$ ) currents.

The outline of the paper is as follows. In Sec. II, we develop the general formalism for the electromagnetic form factors in the SU(3) NJL. In Sec. III, we discuss the electric form factors with related quantities such as electric charge radii. In Sec. IV, we continue to study the magnetic form factors of the SU(3) octet baryons. In Sec. V, we summarize the work and draw conclusions.

## II. THE GENERAL FORMALISM

In this section, we present the general formalism for the electromagnetic form factors of the SU(3) octet baryons in the NJL.

The SU(3) NJL is characterized by a partition function in Euclidean space given by the functional integral over pseudoscalar meson and quark fields:

$$\begin{aligned} \mathcal{Z} &= \int \mathcal{D}\Psi \mathcal{D}\Psi^\dagger \mathcal{D}\pi^a \exp(-S_{\text{NJL}}) \\ &= \int \mathcal{D}\Psi \mathcal{D}\Psi^\dagger \mathcal{D}\pi^a \exp\left(-\int d^4x \Psi^\dagger iD\Psi\right), \end{aligned} \quad (1)$$

where  $D$  denotes the Dirac differential operator

$$iD = \beta(-i\partial + \hat{m} + MU) \quad (2)$$

with the pseudoscalar chiral field

$$U = \exp i\pi^a \lambda^a \gamma_5. \quad (3)$$

$\hat{m}$  is the matrix of the current quark mass given by

$$\hat{m} = \text{diag}(m_u, m_d, m_s) = m_0 \mathbf{1} + m_8 \lambda_8. \quad (4)$$

$\lambda^a$  represent the usual Gell-Mann matrices normalized as  $\text{tr}(\lambda^a \lambda^b) = 2\delta^{ab}$ . Here, we assume isospin symmetry, i.e.,  $m_u = m_d$ .  $M$  shows the dynamical quark mass arising from the spontaneous chiral symmetry breaking, which is in general momentum dependent [4]. For the sake of convenience,

we shall look upon  $M$  as a constant and introduce the ultra-violet cutoff via the proper time regularization which preserves gauge and chiral invariance [29]. The  $m_0$  and  $m_8$  in Eq. (4) are, respectively, defined by

$$m_0 = \frac{m_u + m_d + m_s}{3}, \quad m_8 = \frac{m_u + m_d - 2m_s}{2\sqrt{3}}. \quad (5)$$

The operator  $iD$  is expressed in Euclidean space in terms of the Euclidean time derivative  $\partial_\tau$  and the Dirac one-particle Hamiltonian  $H(U)$

$$iD = \partial_\tau + H(U) + \beta \hat{m} - \beta \bar{m} \mathbf{1} \quad (6)$$

with

$$H(U) = \frac{\vec{\alpha} \cdot \nabla}{i} + \beta M U + \beta \bar{m} \mathbf{1}. \quad (7)$$

$\beta$  and  $\vec{\alpha}$  are the well-known Dirac Hermitian matrices [30]. The  $\bar{m}$  is defined by  $(m_u + m_d)/2 = m_u = m_d$ . We want to emphasize that the NJL model is a low-energy effective model of QCD. Hence, the action of this model can have, in principle, corrections from higher orders such as a term  $\sim m^2 \Psi^\dagger \Psi$  for example. However, the coefficient in front of such a term is not known<sup>1</sup> theoretically. Therefore, it is meaningless to go beyond the linear order of the quark mass expansion unless higher order corrections (e.g., the coefficient in front of  $\hat{m}^2 \Psi^\dagger \Psi$ ) to the action are known.

The electromagnetic form factors of the baryons  $F_i(q^2)$  are defined by the expectation values of the electromagnetic current  $V_\mu$  of the quark fields:

$$\begin{aligned} \langle B', p' | V_\mu(0) | B, p \rangle &= \bar{u}_{B'}(p') \left[ \gamma_\mu F_1(q^2) \right. \\ &\quad \left. + i \sigma_{\mu\nu} \frac{q^\nu}{2M_N} F_2(q^2) \right] u_B(p) \end{aligned} \quad (8)$$

with

$$V_\mu(z) = \bar{\Psi}(z) \gamma_\mu \hat{Q} \Psi(z). \quad (9)$$

$M_N$  denotes the nucleon mass.  $\hat{Q}$  designates the charge operator of the quark field  $\Psi(z)$ :

$$\hat{Q} = \begin{pmatrix} \frac{2}{3} & 0 & 0 \\ 0 & -\frac{1}{3} & 0 \\ 0 & 0 & -\frac{1}{3} \end{pmatrix} = T_3 + \frac{Y}{2}. \quad (10)$$

$T_3$  and  $Y$  are, respectively, the third component of the isospin and hypercharge given by the Gell-Mann–Nishijima formula. The  $q^2$  is just the four-momentum transfer  $q^2 = -Q^2$  with

<sup>1</sup>The coefficient for the  $\hat{m}^2 \Psi^\dagger \Psi$  is determined by the soft-pion theorem.

$Q^2 > 0$ . Hence, the electromagnetic current  $V_\mu$  can be decomposed into the third and eighth SU(3) octet currents

$$V_\mu = V_\mu^{(3)} + \frac{1}{\sqrt{3}} V_\mu^{(8)} \quad (11)$$

with

$$V_\mu^{(3)} = \frac{1}{2} \bar{\Psi} \gamma_\mu \lambda^3 \Psi, \quad V_\mu^{(8)} = \frac{1}{2} \bar{\Psi} \gamma_\mu \lambda^8 \Psi. \quad (12)$$

The electromagnetic form factors  $F_i(Q^2)$  can be expressed in terms of the Sachs form factors,  $G_E(Q^2)$  and  $G_M(Q^2)$ :

$$G_E^B(Q^2) = F_1^B(Q^2) - \frac{Q^2}{4M_N^2} F_2^B(Q^2),$$

$$G_M^B(Q^2) = F_1^B(Q^2) + F_2^B(Q^2). \quad (13)$$

In the nonrelativistic limit ( $Q^2 \ll M_N^2$ ), the Sachs form factors  $G_E(Q^2)$  and  $G_M(Q^2)$  are related to the time and space components of the electromagnetic current, respectively:

$$\langle B', p' | V_0(0) | B, p \rangle = G_E^B(Q^2)$$

$$\langle B', p' | V_i(0) | B, p \rangle = \frac{1}{2M_N} G_M^B(Q^2) i \epsilon_{ijk} q^j \langle \lambda' | \sigma_k | \lambda \rangle, \quad (14)$$

where  $\sigma_k$  stand for Pauli spin matrices.  $|\lambda\rangle$  is the corresponding spin state of the baryon.

The matrix elements of the electromagnetic current can be represented by the Euclidean functional integral in our model defined by Eq. (1):

$$\begin{aligned} \langle B', p' | V_\mu(0) | B, p \rangle &= \frac{1}{\mathcal{L}_{T \rightarrow \infty}} \lim_{T \rightarrow \infty} \exp\left(ip_4 \frac{T}{2} - ip'_4 \frac{T}{2}\right) \int d^3x d^3y \exp(-i\vec{p}' \cdot \vec{y} + i\vec{p} \cdot \vec{x}) \\ &\times \int \mathcal{D}U \int \mathcal{D}\Psi \int \mathcal{D}\Psi^\dagger J_{B'}(\vec{y}, T/2) \Psi^\dagger(0) \beta \gamma_\mu \hat{Q} \Psi(0) J_B^\dagger(\vec{x}, -T/2) \exp\left[-\int d^4z \Psi^\dagger iD\Psi\right]. \end{aligned} \quad (15)$$

The baryonic states  $|B, p\rangle$  and  $\langle B', p'|$  are, respectively, defined by

$$\begin{aligned} |B, p\rangle &= \lim_{x_4 \rightarrow -\infty} \exp(ip_4 x_4) \frac{1}{\sqrt{Z}} \int d^3x \exp(i\vec{p} \cdot \vec{x}) J_B^\dagger(\vec{x}, x_4) |0\rangle \\ \langle B', p'| &= \lim_{y_4 \rightarrow +\infty} \exp(-ip'_4 y_4) \frac{1}{\sqrt{Z}} \int d^3y \exp(-i\vec{p}' \cdot \vec{y}) \langle 0 | J_{B'}(\vec{y}, y_4). \end{aligned} \quad (16)$$

The baryon current  $J_B$  can be constructed from quark fields with the number of colors  $N_c$ :

$$J_B(x) = \frac{1}{N_c!} \epsilon_{i_1 \dots i_{N_c}} \Gamma_{JJ_3 TT_3 Y}^{\alpha_1 \dots \alpha_{N_c}} \psi_{\alpha_1 i_1}(x) \dots \psi_{\alpha_{N_c} i_{N_c}}(x). \quad (17)$$

$\alpha_1 \dots \alpha_{N_c}$  denote spin-flavor indices, while  $i_1 \dots i_{N_c}$  designate color indices. The matrices  $\Gamma_{JJ_3 TT_3 Y}^{\alpha_1 \dots \alpha_{N_c}}$  are taken to endow the corresponding current with the quantum numbers  $JJ_3 TT_3 Y$ . The  $J_B^\dagger$  plays the role of creating the baryon state. With the quark fields being integrated out, Eq. (15) can be divided into two separate contributions:

$$\langle B', p' | V_\mu(0) | B, p \rangle = \langle B', p' | V_\mu(0) | B, p \rangle_{\text{val}} + \langle B', p' | V_\mu(0) | B, p \rangle_{\text{sea}}, \quad (18)$$

where

$$\begin{aligned} \langle B', p' | V_\mu(0) | B, p \rangle_{\text{val}} &= \frac{1}{\mathcal{L}} \Gamma_{J'J'_3 T' T'_3 Y'}^{\beta_1 \dots \beta_{N_c}} \Gamma_{JJ_3 TT_3 Y}^{\alpha_1 \dots \alpha_{N_c}^*} \lim_{T \rightarrow \infty} \exp\left(ip_4 \frac{T}{2} - ip'_4 \frac{T}{2}\right) \int d^3x d^3y \exp(-i\vec{p}' \cdot \vec{y} + i\vec{p} \cdot \vec{x}) \\ &\times \int \mathcal{D}U \exp(-S_{\text{eff}}) \sum_{i=1}^{N_c} \beta_i \left\langle \vec{y}, T/2 \left| \frac{1}{iD} \right| 0, t_z \right\rangle_{\gamma} [\beta \gamma_\mu \hat{Q}]_{\gamma \gamma' \gamma'} \left\langle 0, t_z \left| \frac{1}{iD} \right| \vec{x}, -T/2 \right\rangle_{\alpha_i} \\ &\times \prod_{j \neq i}^{N_c} \beta_j \left\langle \vec{y}, T/2 \left| \frac{1}{iD} \right| \vec{x}, -T/2 \right\rangle_{\alpha_j} \end{aligned} \quad (19)$$

and

$$\begin{aligned} \langle B', p' | V_\mu(0) | B, p \rangle_{\text{sea}} &= \frac{1}{\mathcal{Z}} \Gamma_{J'J'_3T'T'_3Y'}^{\beta_1 \cdots \beta_{N_c}} \Gamma_{JJ_3TT_3Y}^{\alpha_1 \cdots \alpha_{N_c}^*} \lim_{T \rightarrow \infty} \exp\left(ip_4 \frac{T}{2} - ip'_4 \frac{T}{2}\right) \int d^3x d^3y \exp(-i\vec{p}' \cdot \vec{y} + i\vec{p} \cdot \vec{x}) \\ &\times \int \mathcal{D}U \exp(-S_{\text{eff}}) \text{Tr}_{\gamma\lambda c} \left\langle 0, t_z \left| \frac{1}{iD} [\beta \gamma_\mu \hat{Q}] \right| 0, t_z \right\rangle \prod_{i=1}^{N_c} \beta_i \left\langle \vec{y}, T/2 \left| \frac{1}{iD} \vec{x}, -T/2 \right\rangle_{\alpha_i} \right. \end{aligned} \quad (20)$$

$S_{\text{eff}}$  is the effective chiral action expressed by

$$S_{\text{eff}} = -\text{Sp} \ln[\partial_\tau + H(U) + \beta \hat{m} - \beta \bar{m} \mathbf{1}]. \quad (21)$$

Sp stands for the functional trace of the time-independent function.

The integral over bosonic fields can be carried out by the saddle point method in the large  $N_c$  limit, choosing the following ansatz:

$$U = \begin{pmatrix} U_0 & 0 \\ 0 & 1 \end{pmatrix}, \quad (22)$$

where  $U_0$  is the SU(2) chiral background field

$$U_0 = \exp[\vec{n} \cdot \vec{\tau} P(r)]. \quad (23)$$

$P(r)$  denotes the profile function satisfying the boundary condition  $P(0) = \pi$  and  $P(\infty) = 0$ . In order to find the quantum  $1/N_c$  corrections, we have to integrate Eqs. (19), (20) over small oscillations of the pseudo-Goldstone field (22) around the saddle point. This will not be done except for the zero modes. The corresponding fluctuations of the pion fields are not small and hence cannot be neglected. The zero modes are pertinent to continuous symmetries in our problem. Actually, there are three translational and seven rotational zero modes. We have to take into account the translational zero modes properly in order to evaluate form factors, since the soliton is not invariant under translation and its translational invariance is restored only after integrating over the translational zero modes. The rotational zero modes determine the quantum numbers of baryons [9]. Explicitly, the zero modes are taken into account by considering a slowly *rotating* and *translating* hedgehog:

$$\tilde{U}(\vec{x}, t) = A(t) U[\vec{x} - \vec{Z}(t)] A^\dagger(t). \quad (24)$$

$A(t)$  belongs to an SU(3) unitary matrix. The Dirac operator  $i\tilde{D}$  in Eq. (6) can be written as

$$\begin{aligned} i\tilde{D} &= [\partial_\tau + H(U) + A^\dagger(t) \dot{A}(t) - i\beta \vec{Z} \cdot \nabla \\ &+ \beta A^\dagger(t) (\hat{m} - \bar{m} \mathbf{1}) A(t)]. \end{aligned} \quad (25)$$

The corresponding collective action is expressed by

$$\begin{aligned} \tilde{S}_{\text{eff}} &= -N_c \text{Sp} \ln[\partial_\tau + H(U) + A^\dagger(t) \dot{A}(t) - i\beta \vec{Z} \cdot \nabla + \beta A^\dagger(t) \\ &\times (\hat{m} - \bar{m} \mathbf{1}) A(t) - \beta A^\dagger(t) V_\mu \gamma_\mu \hat{Q} A(t)] \end{aligned} \quad (26)$$

with the angular velocity

$$A^\dagger(t) \dot{A}(t) = i\Omega_E = \frac{1}{2} i\Omega_E^a \lambda^a \quad (27)$$

and the velocity of the translational motion

$$\dot{\vec{Z}} = \frac{d}{dt} \vec{Z}. \quad (28)$$

The canonical quantization of the SU(3) soliton can be found in Refs. [31,32]. Expanding Eq. (26) in powers of angular and translational velocities ( $\sim 1/N_c$ ), we end up with the action for collective coordinates:

$$S_{\text{coll}} \approx -N_c \text{Tr} \ln iD + S_{\text{rot}}[A] + S_{\text{trans}}[\vec{Z}], \quad (29)$$

where

$$S_{\text{rot}}[A] = \frac{1}{2} I_{ab} \int dt \Omega_a \Omega_b, \quad S_{\text{trans}}[\vec{Z}] = \frac{1}{2} M_{cl} \int dt \dot{\vec{Z}} \cdot \dot{\vec{Z}}, \quad (30)$$

with the moments of inertia  $I^{ab}$  calculated in Ref. [23].  $M_{cl}$  is a classical mass of the soliton. Corresponding collective Hamiltonians have a form

$$H_{\text{rot}} = (I^{-1})_{ab} J_a J_b, \quad H_{\text{trans}} = \frac{\vec{P} \cdot \vec{P}}{2M_{cl}}, \quad (31)$$

where  $J_a$  are operators of angular momentum and  $\vec{P}$  are momentum operators.

Hence, Eqs. (19) and (20) can be written in terms of the rotated Dirac operator  $i\tilde{D}$  and chiral effective action  $\tilde{S}_{\text{eff}}$ . The functional integral over the pseudoscalar field  $U$  is replaced by the path integral which can be calculated in terms of the eigenstates of the Hamiltonian corresponding to the collective action given in Eq. (29) and these Hamiltonians can be diagonalized in an exact manner. Therefore, Eqs. (19) and (20) can be rewritten as ordinary integrals:

$$\begin{aligned}
\langle B', p' | V_\mu(0) | B, p \rangle_{\text{val}} &= \frac{1}{\mathcal{Z}} \Gamma_{JJ_3 T_3 Y}^{\beta_1 \dots \beta_{N_c}} \Gamma_{JJ_3 TT_3 Y}^{\alpha_1 \dots \alpha_{N_c}^*} \exp\{-[(N_c-1)E_{\text{val}} + E_{\text{sea}}]T\} \lim_{T \rightarrow \infty} \int d^3x d^3y \exp(-i\vec{p}' \cdot \vec{y} + i\vec{p} \cdot \vec{x}) \\
&\times \int dA_f dA dA_i d\vec{Z}_f d\vec{Z} d\vec{Z}_i \langle \vec{Z}_f | \exp(-H_{\text{trans}} T/2) | \vec{Z} \rangle \langle \vec{Z} | \exp(-H_{\text{trans}} T/2) | \vec{Z}_i \rangle \langle A_f | \exp(-H_{\text{rot}} T/2) | A \rangle \\
&\times \langle A | \exp(-H_{\text{rot}} T/2) | A_i \rangle \sum_{k=1}^{N_c} \mathcal{S} \left[ \beta_k \left\langle \vec{y} - \vec{Z}_f, T/2 \left| A_f \frac{1}{i\vec{D}} \right| -\vec{Z} \right\rangle_{\gamma} [A^\dagger \beta \gamma_\mu \hat{Q} A]_{\gamma\gamma'} \right. \\
&\times \left. \gamma' \left\langle -\vec{Z} \left| \frac{1}{i\vec{D}} A_i^\dagger \right| \vec{x} - \vec{Z}_i, -T/2 \right\rangle_{\alpha_k} \right], \tag{32}
\end{aligned}$$

$$\begin{aligned}
\langle B', p' | V_\mu(0) | B, p \rangle_{\text{sea}} &= \frac{1}{\mathcal{Z}} \Gamma_{JJ_3 T_3 Y}^{\beta_1 \dots \beta_{N_c}} \Gamma_{JJ_3 TT_3 Y}^{\alpha_1 \dots \alpha_{N_c}^*} \exp[-(N_c E_{\text{val}} + E_{\text{sea}})T] \lim_{T \rightarrow \infty} \int d^3x d^3y \exp(-i\vec{p}' \cdot \vec{y} + i\vec{p} \cdot \vec{x}) \\
&\times \int dA_f dA dA_i d\vec{Z}_f d\vec{Z} d\vec{Z}_i \langle \vec{Z}_f | \exp(-H_{\text{trans}} T/2) | \vec{Z} \rangle \langle \vec{Z} | \exp(-H_{\text{trans}} T/2) | \vec{Z}_i \rangle \langle A_f | \exp(-H_{\text{rot}} T/2) | A \rangle \\
&\times \langle A | \exp(-H_{\text{rot}} T/2) | A_i \rangle \mathcal{S} \left[ \text{Tr}_{\gamma\lambda c} \left\langle -\vec{Z} \left| \frac{1}{i\vec{D}} [A^\dagger \beta \gamma_\mu \hat{Q} A] \right| -\vec{Z} \right\rangle_{\gamma\gamma'} \right]. \tag{33}
\end{aligned}$$

$\mathcal{T}[\dots]$  denotes the time-ordered product of collective operators. This is because of the fact that the functional integral corresponds to the matrix elements of the time-ordered products of the collective operators. In particular, the time ordering is very significant when we consider the magnetic form factors (as in case of the axial constants: see [15,20]), since the spin operator  $J^a$  does not commute with the SU(3) rotational unitary matrix  $A(t)$ . As we integrate over zero modes in the final and initial states, we obtain the translational and rotational corrections of the classical energies of the soliton from the effective actions  $S_{\text{trans}}$  and  $S_{\text{rot}}$ . Therefore, introducing the spectral representations of the quark propagator [5], expressed by the eigenfunctions of the Dirac Hamiltonian  $H(U)$ , and making use of relations

$$\int d\vec{Z}_i \langle \vec{Z} | \exp(-S_{\text{trans}}) | \vec{Z}_i \rangle f(\vec{x} - \vec{Z}_i) \xrightarrow{T \rightarrow \infty} \langle \vec{Z} | \exp(-S_{\text{trans}}) | \vec{x} \rangle \int d^3x' f(\vec{x}'), \tag{34}$$

$$\Gamma_{JJ_3 TT_3 Y}^{\beta_1 \dots \beta_{N_c}} \int d^3\vec{x}' \prod_{k=1}^{N_c} [A_f \phi(\vec{x}')]_{\beta_k} = \psi_{(YTT_3)(Y'JJ_3)}^{(8)*}(A_f), \tag{35}$$

$$\Gamma_{JJ_3 TT_3 Y}^{\alpha_1 \dots \alpha_{N_c}^*} \int d^3\vec{x}' \prod_{k=1}^{N_c} [\phi^\dagger(\vec{x}') A_i^\dagger]_{\alpha_k} = \psi_{(YTT_3)(Y'JJ_3)}^{(8)}(A_i), \tag{36}$$

$$\langle A | \exp(-S_{\text{rot}}) | A_i \rangle = \sum_{\substack{n \\ (YTT_3) \\ (Y'JJ_3)}} \psi_{(YTT_3)(Y'JJ_3)}^{(n)}(A) \psi_{(YTT_3)(Y'JJ_3)}^{(n)*}(A_i) \exp\left(-\frac{J(J+1)}{2I} \Gamma\right), \tag{37}$$

we obtain relatively simple expressions:

$$\langle B', p' | V_\mu(0) | B, p \rangle_{\text{val}} = N_c \int d^3Z \exp(i\vec{q} \cdot \vec{Z}) \int_{\text{SU}(3)} dA \psi_{\mu\nu}^{(n)*}(A) \psi_{\mu'\nu'}^{(n)}(A) \mathcal{S}[\mathcal{F}_1^{(\Omega^0)}(A) + \mathcal{F}_2^{(\Omega^1)}(A) + \mathcal{F}_3^{(m_s)}(A)], \tag{38}$$

$$\langle B', p' | V_\mu(0) | B, p \rangle_{\text{sea}} = N_c \int d^3Z \exp(i\vec{q} \cdot \vec{Z}) \int_{\text{SU}(3)} dA \psi_{\mu\nu}^{(n)*}(A) \psi_{\mu'\nu'}^{(n)}(A) \mathcal{S} \left[ \text{Tr} \left\langle \vec{Z} \left| \frac{1}{i\vec{D}} [A^\dagger \beta \gamma_\mu \hat{Q} A] \right| \vec{Z} \right\rangle \right]. \tag{39}$$

Here, we have considered contributions up to the first order of  $\Omega_E$ , i.e., the  $1/N_c$  corrections and the linear corrections of the strange quark mass  $m_s$ . The mixed term  $O(m_s/N_c)$  is relatively small, so that it is neglected [28]. It is performed by the expansion of the propagator  $1/i\vec{D}$  in terms of  $\Omega_E$  and  $m_s$ :

$$\frac{1}{i\tilde{D}} \approx \frac{1}{\partial_\tau + H} + \frac{1}{\partial_\tau + H} (-i\Omega_E) \frac{1}{\partial_\tau + H} + \frac{1}{\partial_\tau + H} (-\beta A^\dagger \hat{m} A) \frac{1}{\partial_\tau + H}. \quad (40)$$

The collective SU(3) octet wave functions  $\psi_{\mu'\nu}^{(n)}(A)$  are identified with the SU(3) Wigner functions

$$\psi_{(YTT_3)(Y'JJ_3)}^{(n)}(A) = \sqrt{\dim(n)} (-1)^{Y'/2+J_3} [\langle Y, T, T_3 | D^{(n)}(A) | -Y', J, -J_3 \rangle]^* \quad (41)$$

as eigenstates of the collective rotational Hamiltonian. The functions  $\mathcal{F}_i(A)$  are defined as

$$\mathcal{F}_1^{(\Omega^0)}(A) = \langle \text{val} | \beta \gamma_\mu \lambda^a | \text{val} \rangle D_{Qa}^{(8)}(A),$$

$$\mathcal{F}_2^{(\Omega^1)}(A) = - \sum_n [\langle \text{val} | \lambda^a | n \rangle \langle n | \beta \gamma_\mu \lambda^b | \text{val} \rangle i\Omega_E^a(A) D_{Qb}^{(8)}(A) \langle \text{val} | \beta \gamma_\mu \lambda^b | n \rangle \langle n | \lambda^a | \text{val} \rangle D_{Qb}^{(8)}(A) i\Omega_E^a(A)] \frac{1}{E_{\text{val}} - E_n},$$

$$\begin{aligned} \mathcal{F}_3^{(m_s)}(A) = & -(m_0 - \bar{m}) \sum_n [\langle \text{val} | \beta | n \rangle \langle n | \beta \gamma_\mu \lambda^a | \text{val} \rangle D_{Qa}^{(8)}(A) \langle \text{val} | \beta \gamma_\mu \lambda^a | n \rangle \langle n | \beta | \text{val} \rangle D_{Qa}^{(8)}(A)] \frac{1}{E_{\text{val}} - E_n} \\ & - m_8 \sum_n [\langle \text{val} | \beta \lambda^a | n \rangle \langle n | \beta \gamma_\mu \lambda^b | \text{val} \rangle D_{8a}^{(8)}(A) D_{Qb}^{(8)}(A) + \langle \text{val} | \beta \gamma_\mu \lambda^b | n \rangle \langle n | \beta \lambda^a | \text{val} \rangle D_{Qb}^{(8)}(A) D_{8a}^{(8)}(A)] \frac{1}{E_{\text{val}} - E_n}. \end{aligned} \quad (42)$$

$D_{Qa}^{(8)}$  is defined as  $\frac{1}{2}(D_{3a}^{(8)} + 1/\sqrt{3} D_{8a}^{(8)})$ . The collective SU(3) octet wave function in Eq. (41) satisfies the orthonormality [33]

$$\int dA \psi_{\mu'\nu'}^{(n')*}(A) \psi_{\mu\nu}^{(n)}(A) = \delta_{n'n} \delta_{\mu'\mu} \delta_{\nu'\nu}. \quad (43)$$

The subscripts  $\mu\nu$  of  $\psi_{\mu\nu}^{(n)}$  represent  $(YTT_3)(Y'JJ_3)$ . ( $n$ ) stands for the irreducible representation of SU(3).  $Y'$  is the negative of the right hypercharge constrained by  $Y_R = N_c B/3 = 1$ . Since Eq. (39), in particular, its real part diverges, we have to regularize it. We employ the well-known proper time regularization

$$\text{Re}S_{\text{eff}} = \frac{1}{2} \text{Tr} \int_0^\infty \frac{du}{u} e^{-uD^\dagger D} \phi(u; \Lambda_i) \quad (44)$$

with

$$\phi(u; \Lambda_i) = \sum_i c_i \theta\left(u - \frac{1}{\Lambda_i^2}\right). \quad (45)$$

The cutoff parameter  $\phi(u; \Lambda_i)$  is fixed via reproducing the physical pion decay constant  $f_\pi = 93$  MeV and other mesonic properties [23]. As was done in case of the valence part, we take into account the  $1/N_c$  and linear  $m_s$  corrections (see Appendix A for detail).

Making use of the expansion equation (40) and the SU(3) octet wave functions and employing the proper-time regularization, we arrive at

$$\begin{aligned} \langle B', p' | V_\mu(0) | B, p \rangle_{\text{val}} = & N_c \langle D_{Qa}^{(8)} \rangle_B \mathcal{P}_{\mu; \text{val}}^a(\vec{q}) + \frac{N_c}{2} \sum_m \left\{ \frac{\text{sgn}(E_m) \langle [D_{Qa}^{(8)}, i\Omega_E^b] \rangle_B \delta_{\mu i}}{\langle \{D_{Qa}^{(8)}, i\Omega_E^b\} \rangle_B \delta_{\mu 4}} \right\} \frac{\mathcal{Q}_{\mu; \text{val}, m}^{ab}(\vec{q})}{E_n - E_{\text{val}}} \\ & + \frac{N_c}{2} \sum_m \langle \{D_{Qa}^{(8)}, i\Omega_E^b\} \rangle_B \delta_{\mu i} \frac{\mathcal{Q}_{\mu; \text{val}, m}^{ab}(\vec{q})}{E_n - E_{\text{val}}} + N_c (m_0 - \bar{m}) \sum_m \langle D_{Qa}^{(8)} \rangle_B \delta_{\mu i} \frac{\mathcal{M}_{\mu; \text{val}, m}^a(\vec{q})}{E_n - E_{\text{val}}} \\ & + N_c m_8 \sum_m \langle \{D_{Qa}^{(8)}, D_{8b}^{(8)}\} \rangle_B \frac{\mathcal{H}_{\mu; \text{val}, m}^{ab}(\vec{q})}{E_n - E_{\text{val}}}, \end{aligned} \quad (46)$$

$$\begin{aligned}
\langle B', p' | V_\mu(0) | B, p \rangle_{\text{sea}} = & -\frac{N_c}{2} \sum_m \text{sgn}(E_n) \langle D_{Qa/B}^{(8)} \left\{ \begin{array}{c} \mathcal{R}(E_n) \delta_{\mu i} \\ \delta_{\mu 4} \end{array} \right\} \mathcal{P}_{\mu;n}^a(\vec{q}) \\
& + \frac{N_c}{4} \sum_{n,m} \left\{ \begin{array}{c} \mathcal{R}_Q(E_n, E_m) \langle [D_{Qa}^{(8)}, i\Omega_E^b] \rangle_B \delta_{\mu i} \\ \mathcal{R}_I(E_n, E_m) \langle \{D_{Qa}^{(8)}, i\Omega_E^b\} \rangle_B \delta_{\mu 4} \end{array} \right\} \mathcal{Q}_{\mu;nm}^{ab}(\vec{q}) \\
& + \frac{N_c}{4} \sum_{n,m} \langle \{D_{Qa}^{(8)}, i\Omega_E^b\} \rangle_B \mathcal{R}_M(E_n, E_m) \delta_{\mu i} \mathcal{M}_{\mu;nm}^{ab}(\vec{q}) \\
& + \frac{N_c}{2} (m_0 - \bar{m}) \sum_{n,m} \langle D_{Qa/B}^{(8)} \rangle_B \mathcal{R}_\beta(E_n, E_m) \mathcal{M}_{\mu;nm}^a(\vec{q}) \delta_{\mu i} \\
& + \frac{N_c}{2} m_8 \sum_{n,m} \langle \{D_{Qa}^{(8)}, D_{8b}^{(8)}\} \rangle_B \left\{ \begin{array}{c} \mathcal{R}_\beta(E_n, E_m) \delta_{\mu i} \\ \mathcal{R}_M(E_n, E_m) \delta_{\mu 4} \end{array} \right\} \mathcal{H}_{\mu;nm}^{ab}(\vec{q}), \tag{47}
\end{aligned}$$

where the quark matrix elements are written as

$$\begin{aligned}
\mathcal{P}_{\mu;n}^a(\vec{q}) &= \int d^3x e^{i\vec{q}\cdot\vec{x}} \Psi_n^\dagger(x) \beta \gamma_\mu \lambda^a \Psi_n(x), \\
\mathcal{Q}_{\mu;nm}^{ab}(\vec{q}) &= \int d^3x e^{i\vec{q}\cdot\vec{x}} \int d^3y \Psi_n^\dagger(x) \beta \gamma_\mu \lambda^a \Psi_m(x) \Psi_m^\dagger(y) \lambda^b \Psi_n(y), \\
\mathcal{M}_{\mu;nm}^a(\vec{q}) &= \int d^3x e^{i\vec{q}\cdot\vec{x}} \int d^3y \Psi_n^\dagger(x) \beta \gamma_\mu \lambda^a \Psi_m(x) \Psi_m^\dagger(y) \beta \Psi_n(y), \\
\mathcal{H}_{\mu;nm}^{ab}(\vec{q}) &= \int d^3x e^{i\vec{q}\cdot\vec{x}} \int d^3y \Psi_n^\dagger(x) \beta \gamma_\mu \lambda^a \Psi_m(x) \Psi_m^\dagger(y) \beta \lambda^b \Psi_n(y). \tag{48}
\end{aligned}$$

The regularization functions are given by

$$\begin{aligned}
\mathcal{R}(E_n) &= \int \frac{du}{\sqrt{\pi u}} \phi(u; \Lambda_i) |E_n| e^{-uE_n^2}, \\
\mathcal{R}_Q(E_n, E_m) &= \frac{1}{2\pi} c_i \int_0^1 d\alpha \frac{\alpha(E_n + E_m) - E_m}{\sqrt{\alpha(1-\alpha)}} \frac{\exp\{-[\alpha E_n^2 + (1-\alpha)E_m^2]/\Lambda_i^2\}}{\alpha E_n^2 + (1-\alpha)E_m^2}, \\
\mathcal{R}_I(E_n, E_m) &= -\frac{1}{2\sqrt{\pi}} \int_0^\infty \frac{du}{\sqrt{u}} \phi(u; \Lambda_i) \left[ \frac{E_n e^{-uE_n^2} + E_m e^{-uE_m^2}}{E_n + E_m} + \frac{e^{-uE_n^2} - e^{-uE_m^2}}{u(E_n^2 - E_m^2)} \right], \\
\mathcal{R}_M(E_n, E_m) &= \frac{1}{2} \frac{\text{sgn}(E_n) - \text{sgn}(E_m)}{E_n - E_m}, \\
\mathcal{R}_\beta(E_n, E_m) &= \frac{1}{2\sqrt{\pi}} \int_0^\infty \frac{du}{\sqrt{u}} \phi(u; \Lambda_i) \left[ \frac{E_n e^{-uE_n^2} - E_m e^{-uE_m^2}}{E_n - E_m} \right]. \tag{49}
\end{aligned}$$

$I_i$  are moments of inertia defined in Ref. [22].  $\langle \rangle_B$  denotes the expectation value of the Wigner  $D$  functions in collective space spanned by  $A$ . The expectation values of the  $D$  functions can be evaluated by SU(3) Clebsch-Gordan coefficients listed in [33,34]. The index  $\mu$  is the Lorentz index and  $a$  and  $b$  denote the flavors, whereas  $i$  designates the space component of the electromagnetic current. We can here notice that in Eq. (47)  $1/N_c$  term includes two different commuting relations, i.e., the commutator and anti-commutator between

the SU(3) Wigner function  $D^{(8)}$  and the angular velocity  $\Omega_E$  of the soliton. This is because of the time ordering of the operators and the symmetric properties of the quark matrix elements under indices  $n$  and  $m$  or under  $G^{75}$  parity [35]. If the quark matrix elements are antisymmetric, then the commutator survives, while if they are symmetric, then the anti-commutator does. The quark matrix elements for the electric form factors ( $\mu=4$ ) are symmetric whereas some of the matrix elements for the magnetic form factors are anti-

symmetric. However, note that on the whole the matrix element of the current is symmetric, since the regularization functions are symmetric under exchange of  $n$  and  $m$  except for  $\mathcal{R}_Q$ .

The regularization functions in Eq. (49) are determined in the proper time regularization manifestly except for  $\mathcal{R}_M$  which corresponds to the Wess-Zumino terms from the imaginary part of the action. In fact,  $\mathcal{R}_M$  is not a regularization function. It is independent of the cutoff parameter  $\Lambda$ .

With SU(3) symmetry explicitly broken by  $m_s$ , the collective Hamiltonian is no longer SU(3) symmetric. Therefore, the eigenstates of the Hamiltonian are neither in a pure octet nor in a pure decuplet but in mixed states. Treating  $m_s$  as a perturbation, we can obtain the mixed SU(3) baryonic states:

$$|8, B\rangle = |8, B\rangle + c_{10}^B |\bar{10}, B\rangle + c_{27}^B |27, B\rangle \quad (50)$$

with

$$c_{10}^B = \frac{\sqrt{5}}{15} (\sigma - r_1) \begin{bmatrix} 1 \\ 0 \\ 1 \\ 0 \end{bmatrix} I_2 m_s, \quad (51)$$

$$c_{27}^B = \frac{1}{75} (3\sigma + r_1 - 4r_2) \begin{bmatrix} \sqrt{6} \\ 3 \\ 2 \\ \sqrt{6} \end{bmatrix} I_2 m_s$$

in the basis  $[N, \Lambda, \Sigma, \Xi]$ . Here,  $B$  denotes the SU(3) octet baryons with the spin 1/2. The constant  $\sigma$  is related to the SU(2)  $\pi N$   $\sigma$  term  $\Sigma_{\text{SU}(2)} = 3/2(m_u + m_d)\sigma$  and  $r_i$  designates  $K_i/I_i$ , where  $K_i$  stands for the anomalous moments of inertia defined in Ref. [23].

### III. THE ELECTRIC PROPERTIES OF THE SU(3) OCTET BARYONS

The electric form factors are easily obtained by the matrix elements of the time component of the electromagnetic current, as was defined in Eq. (14). Equation (47) furnishes the final expression of the electric form factor. Since the SU(3)

hedgehog solutions are obtained by means of the embedding of the SU(2) hedgehog field  $U_0$  as shown in Eq. (22), it is convenient to define the projection operators  $P_T$  and  $P_S$ :

$$P_T = \begin{pmatrix} 1 & 0 & 0 \\ 0 & 1 & 0 \\ 0 & 0 & 0 \end{pmatrix}, \quad P_S = \begin{pmatrix} 0 & 0 & 0 \\ 0 & 0 & 0 \\ 0 & 0 & 1 \end{pmatrix}. \quad (52)$$

Having defined these projection operators, we can separate the pure SU(2) part from the SU(3) which are represented by the collective operators. Utilizing the projection operators and introducing SU(2)<sub>T</sub> × U(1)<sub>Y</sub>-invariant tensors

$$P_T \lambda^a = \begin{cases} \tau^a & \text{if } a = 1, 2, 3, \\ 0 & \text{if } a = 4, 5, 6, 7, \\ 1 & \text{if } a = 8, \end{cases}$$

$$P_T \lambda^a P_S \lambda^b = \left[ i(f^{abc} - \epsilon^{abc}) - \frac{1}{\sqrt{3}} (\delta^{ac} \delta^{b8} + \delta^{a8} \delta^{bc}) + d^{abc} \right] \lambda^c, \quad (53)$$

we can find that the quark matrix elements include only the pure SU(2) components with transition matrix elements between the vacuum states with SU(2) flavors and the eigenstates of the one-body Hamiltonian equation (7). The SU(3) elements only appear in the collective parts. Hence, we can write the expression of the electric form factors

$$G_E^B(\vec{Q}^2) = \frac{N_c}{\sqrt{3}} \langle D_{Q8}^{(8)} \rangle_B \mathcal{B}(\vec{Q}^2) - \langle D_{Qa}^{(8)} J_a \rangle_B \frac{2\mathcal{F}_1(\vec{Q}^2)}{I_1} - \langle D_{Qp}^{(8)} J_p \rangle_B \frac{2\mathcal{F}_2(\vec{Q}^2)}{I_2} + \langle D_{8a}^{(8)} D_{Qa}^{(8)} \rangle_B \times \frac{4m_s}{I_1 \sqrt{3}} (I_1 \mathcal{H}_1(\vec{Q}^2) - \mathcal{F}_1(\vec{Q}^2) K_1) + \langle D_{8p}^{(8)} D_{Qp}^{(8)} \rangle_B \times \frac{4m_s}{I_2 \sqrt{3}} (I_2 \mathcal{H}_2(\vec{Q}^2) - \mathcal{F}_2(\vec{Q}^2) K_2), \quad (54)$$

where

$$\mathcal{B}(\vec{Q}^2) = \int d^3x j_0(Qr) \left[ \Psi_{\text{val}}^\dagger(x) \Psi_{\text{val}}(x) - \frac{1}{2} \sum_n \text{sgn}(E_n) \Psi_n^\dagger(x) \Psi_n(x) \right],$$

$$\mathcal{F}_1(\vec{Q}^2) = \frac{N_c}{6} \sum_{n,m} \int d^3x j_0(Qr) \int d^3y \left[ \frac{\Psi_n^\dagger(x) \vec{\tau} \Psi_{\text{val}}(x) \cdot \Psi_{\text{val}}^\dagger(y) \vec{\tau} \Psi_n(y)}{E_n - E_{\text{val}}} + \frac{1}{2} \Psi_n^\dagger(x) \vec{\tau} \Psi_m(x) \cdot \Psi_m^\dagger(y) \vec{\tau} \Psi_n(y) \mathcal{R}_{\mathcal{F}}(E_n, E_m) \right],$$

$$\mathcal{F}_2(\vec{Q}^2) = \frac{N_c}{6} \sum_{n,m^0} \int d^3x j_0(Qr) \int d^3y \left[ \frac{\Psi_{m^0}^\dagger(x) \Psi_{\text{val}}(x) \Psi_{\text{val}}^\dagger(y) \Psi_{m^0}(y)}{E_{m^0} - E_{\text{val}}} + \frac{1}{2} \Psi_n^\dagger(x) \Psi_{m^0}(x) \Psi_{m^0}^\dagger(y) \Psi_n(y) \mathcal{R}_{\mathcal{F}}(E_n, E_{m^0}^0) \right],$$



$$\begin{aligned}
\mathcal{H}_1(\vec{Q}^2) &= \frac{N_c}{6} \sum_{n,m} \int d^3x j_0(Qr) \int d^3y \left[ \frac{\Psi_n^\dagger(x) \vec{\tau} \Psi_{\text{val}}(x) \cdot \Psi_{\text{val}}^\dagger(y) \beta \vec{\tau} \Psi_n(y)}{E_n - E_{\text{val}}} \right. \\
&\quad \left. + \frac{1}{2} \Psi_n^\dagger(x) \vec{\tau} \Psi_m(x) \cdot \Psi_m^\dagger(y) \beta \vec{\tau} \Psi_n(y) \mathcal{R}_{\mathcal{M}}(E_n, E_m) \right], \\
\mathcal{H}_2(\vec{Q}^2) &= \frac{N_c}{6} \sum_{n,m^0} \int d^3x j_0(Qr) \int d^3y \left[ \frac{\Psi_{m^0}^\dagger(x) \Psi_{\text{val}}(x) \Psi_{\text{val}}^\dagger(y) \beta \Psi_{m^0}(y)}{E_{m^0} - E_{\text{val}}} + \frac{1}{2} \Psi_n^\dagger(x) \Psi_{m^0}(x) \Psi_{m^0}^\dagger(y) \beta \Psi_n(y) \mathcal{R}_{\mathcal{M}}(E_n, E_{m^0}) \right],
\end{aligned} \tag{55}$$

with the regularization functions  $\mathcal{R}_1$  and  $\mathcal{R}_{\mathcal{M}}$  defined in Eq. (49). The subscripts  $a$  and  $p$  denote the flavor indices  $a=1,2,3$  and  $p=4, \dots, 7$ , respectively, and  $m^0$  denotes the vacuum state with the SU(2) flavor.  $j_0(Qr)$  is the spherical Bessel function of integral order 0. We can see that when  $\vec{Q}^2=0$ ,  $\mathcal{B}$  becomes the baryon number  $B=1$ , while  $\mathcal{T}_i$  and  $\mathcal{H}_i$  become the usual and the anomalous moments of inertia, respectively. In that case, Eq. (54) is reduced to the Gell-Mann–Nishijima formula  $Q=T_3+\frac{1}{2}Y$ , using the relation

$$\sum_{a=1}^8 D_{3a}^{(8)} R^a = L_3 = T_3, \quad \sum_{a=1}^8 D_{8a}^{(8)} R^a = L_8 = \frac{1}{2} \sqrt{3} Y. \tag{56}$$

At  $\vec{Q}^2=0$ , the mass corrections do not contribute to the electric form factors, since the fourth and fifth terms in Eq. (54) vanish at the zero momentum transfer.

In order to calculate the form factors and other observables numerically, we follow the well-known Kahana and Ripka method [36]. Since the isovector electric charge radii have a pole in the chiral limit, we take the pion mass  $m_\pi = 139$  MeV into account. The self-consistent profile function obtained by the Kahana-Ripka method has a good behavior in the solitonic region, but the tail of the pion field is spoiled a little because of the finite size of the radial box

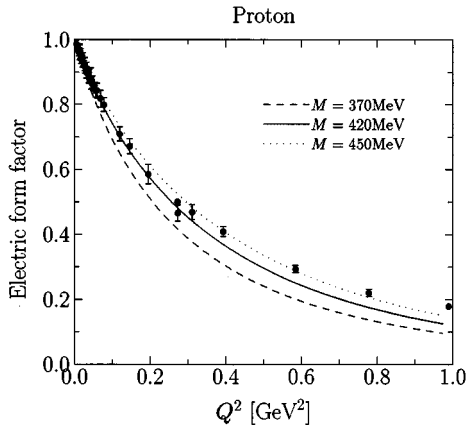


FIG. 1. The proton electric form factor as a function of  $Q^2$ : The dashed curve corresponds to the constituent quark mass  $M=370$  MeV, while solid curve is for  $M=420$  MeV. The dotted curve displays the case of  $M=450$  MeV. The empirical data are taken from Höhler *et al.* [38].

when we take into account the pion mass. Hence, at large distances we use the exact Yukawa-type asymptotic behavior of the profile function:

$$P(r) = \alpha \exp(-m_\pi r) \frac{1 + m_\pi r}{r^2}, \tag{57}$$

where  $\alpha$  is a constant governing the strength of the pion field. It is determined by matching the self-consistent profile function to the asymptotic tail given in Eq. (57) at large distances, i.e., about 4 fm. Since the neutron electric form factor, electromagnetic charge radius, and magnetic form factors are very sensitive to the long-range tail, we have to use the larger size of the radial box. Hence, we employ the box size  $D \approx 10$  fm which is large enough to incorporate the long-range part properly.

Figure 1 shows the electric form factor of the proton while Fig. 2 draws that of the neutron as a function of  $Q^2$  with the constituent quark mass 370 MeV, 420 MeV, and 450 MeV. The empirical data are provided by Ref. [39]. From Fig. 1, we can easily find that the proton electric form factor ( $G_E^p$ ) increases as the constituent quark mass does. For the best fit, we choose the constituent quark mass  $M=420$  MeV

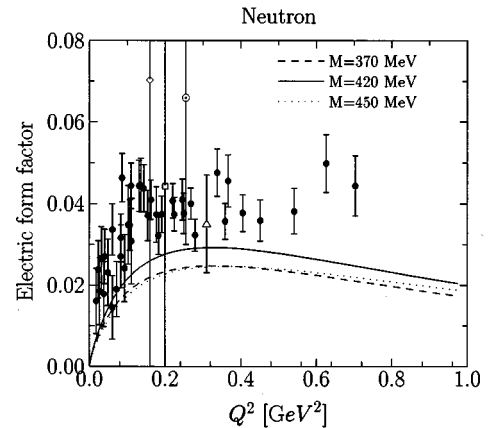


FIG. 2. The neutron electric form factor as a function of  $Q^2$ : The solid curve corresponds to the constituent quark mass  $M=420$  MeV, while dashed curve draws  $M=370$  MeV. The dotted curve displays the case of  $M=450$  MeV. The empirical data are taken from Platchkov *et al.* [39]. The other four points are results for  $G_E^n$  extracted by Jones-Woodward *et al.* [40] (open diamond), by Thompson *et al.* [41] (open box), by Eden *et al.* [42] (open circle), and by Meyerhoff *et al.* [43] (open triangle).

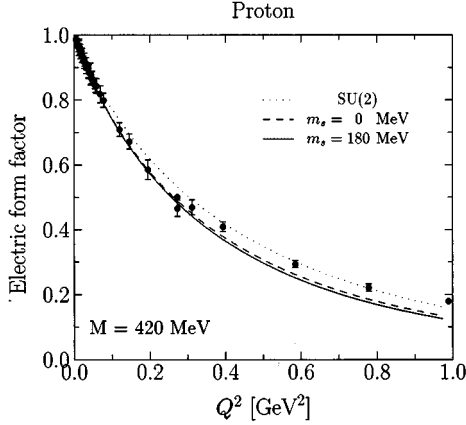


FIG. 3. The proton electric form factor as a function of  $Q^2$ : The solid curve corresponds to the strange quark mass  $m_s = 180$  MeV, while dashed curve draws without  $m_s$ . The dotted curve displays the case of the SU(2) model.  $M = 420$  MeV is chosen for the constituent quark mass. The empirical data are taken from H"ohler *et al.* [38].

as usually done for the other observables. However, the neutron electric form factor ( $G_E^n$ ) does not show such dependence on the  $M$  as that of the proton does. The dependence of  $G_E^n$  is not monotonous. As shown in Fig. 2,  $G_E^n$  with  $M = 420$  MeV is greater than those in the case of  $M = 370$  MeV and  $M = 450$  MeV. At the first glance, it might seem to be strange. However, since  $G_E^n$  is a very tiny and sensitive quantity, one should carefully examine each contribution to it. Having scrutinized each contribution, we find that the wave function corrections given by Eq. (50) are responsible for the above-mentioned behavior in  $G_E^n$ . In particular, the  $\sigma$  appearing in Eq. (51) plays a pivotal role of governing the behavior of  $G_E^n$ . As  $M$  increases, the electric

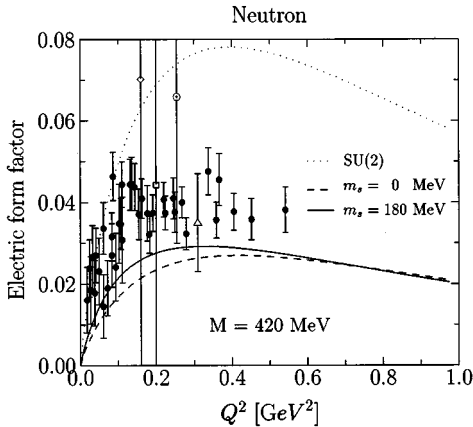


FIG. 4. The neutron electric form factor as a function of  $Q^2$ : The solid curve corresponds to the strange quark mass  $m_s = 180$  MeV, while dashed curve draws without  $m_s$ . The dotted curve displays the case of the SU(2) model.  $M = 420$  MeV is chosen for the constituent quark mass. The empirical data (shaded circle) are taken from Platchkov *et al.* [39]. The other four points are results for  $G_E^n$  extracted by Jones-Woodward *et al.* [40] (open diamond), by Thompson *et al.* [41] (open box), by Eden *et al.* [42] (open circle), and by Meyerhoff *et al.* [43] (open triangle).

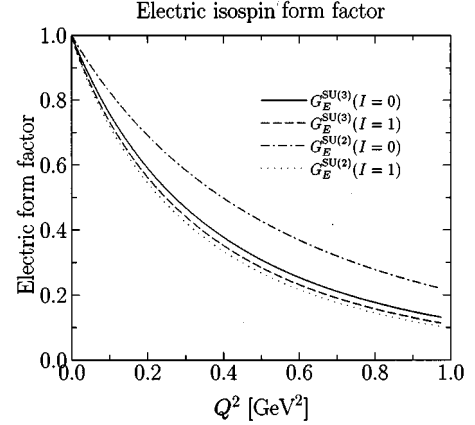


FIG. 5. The electric isospin form factors of the nucleon as a function of  $Q^2$ : The solid curve corresponds to the isoscalar electric form factor of the nucleon in SU(3), while the dashed curve denotes the isovector one. The dot-dashed curve draws the isoscalar one in SU(2), whereas the dotted curve stands for the isovector one in SU(2).

form factors increase but the  $\sigma$  decreases. In the meanwhile, the  $G_E^n$  gets an optimal value around 420 MeV.

The contribution of the  $m_s$  corrections with the wave function corrections is displayed in Figs. 3 and 4. In fact, the  $m_s$  corrections without the collective wave functions modified bring  $G_E^n$  down sizably, since the  $m_s$  terms  $[I_i \mathcal{K}_i(\vec{Q}^2) - \mathcal{I}_i(\vec{Q}^2) K_i]$  diminish electric form factors in general. However, as explained above, the collective wave function corrections are in particular significant in order to improve  $G_E^n$ . On the contrary to the case of the  $G_E^p$  to which the wave function corrections contribute about 1%, those contributions to  $G_E^n$  are strong enough to overcome the  $m_s$  corrections. As a result, the total  $m_s$  corrections enhance  $G_E^n$  about 20% ~ 30% in the small  $Q^2$  region.

More important observables for us are probably electric charge radii which are determined by the behavior of the

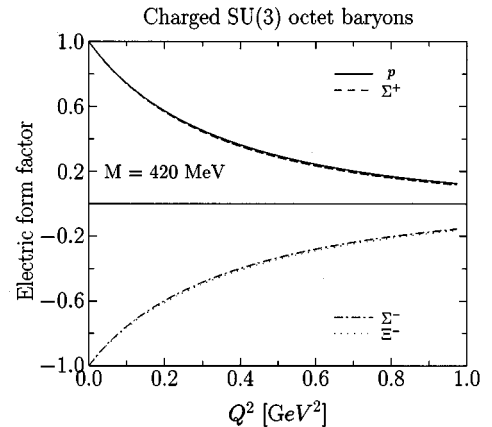


FIG. 6. The electric form factors of the charged SU(3) octet baryons as a function of  $Q^2$ : The solid curve corresponds to the proton electric form factor. The dashed curve is for  $\Sigma^+$ . The dash-dotted curve displays that of  $\Sigma^-$  and the dotted curve that of  $\Xi^-$ .  $M = 420$  MeV is chosen for the constituent quark mass.

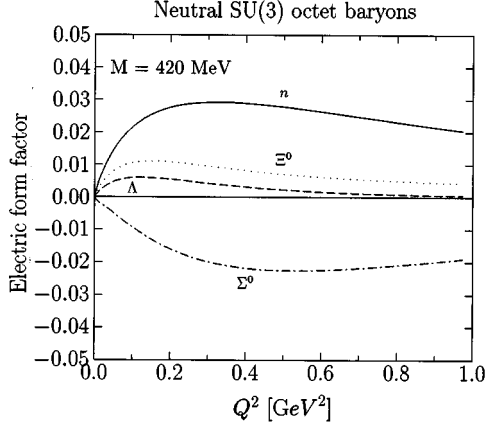


FIG. 7. The electric form factors of the neutral SU(3) octet baryons as a function of  $Q^2$ : The solid curve corresponds to the neutron electric form factor. The dashed curve is for  $\Lambda$ . The dash-dotted curve displays that of  $\Sigma^0$  and the dotted curve that of  $\Xi^0$ .  $M = 420$  MeV is chosen for the constituent quark mass.

electric form factors near  $Q^2=0$ , which are defined by

$$\langle r^2 \rangle_E^B = -6 \left. \frac{dG_E^B(Q^2)}{dQ^2} \right|_{Q^2=0}. \quad (58)$$

Using Eq. (58), we obtain the electric charge radii of the proton and the neutron  $\langle r^2 \rangle_p^{\text{th}} = 0.78 \text{ fm}^2$  and  $\langle r^2 \rangle_n^{\text{th}} = -0.09 \text{ fm}^2$ , respectively. The experimental data are  $\langle r^2 \rangle_p = 0.74 \text{ fm}^2$  and  $\langle r^2 \rangle_n = -0.113 \pm 0.003 \text{ fm}^2$  [44]. We can see that our results are in a good agreement with experimental ones within about 10%.

In dotted curves in Figs. 3 and 4, we show the prediction of the SU(2) model [15]. As for the proton electric form factor, it is comparable to the SU(3), whereas a great discrepancy is observed in case of the neutron electric form factor. This discrepancy can be understood by looking into the electric isospin form factors. Figure 5 shows differences in the electric isospin form factors between the SU(2) and SU(3) models. From Fig. 5, we can find that in case of the SU(3), the difference between the isoscalar and isovector form factors is quite small while their sum is comparable. The discrepancy in the neutron form factors lies in this difference between electric isospin form factors. It is partly because of the absence of  $m_s$  and terms depending on the  $I_2$  in the SU(2) model and partly because of the different expectation

TABLE I. The electric charge radii of the SU(3) octet baryons predicted by our model compared to the evaluation from the Skyrme model by Park and Weigel [37] and the experimental numbers. The constituent quark mass is fixed to  $M = 420$  MeV.

| Baryons    | Our model | Park & Weigel | Experiment |
|------------|-----------|---------------|------------|
| $p$        | 0.78      | 1.20          | 0.74       |
| $n$        | -0.09     | -0.15         | -0.11      |
| $\Lambda$  | -0.04     | -0.06         | -          |
| $\Sigma^+$ | 0.79      | 1.20          | -          |
| $\Sigma^0$ | 0.02      | -0.01         | -          |
| $\Sigma^-$ | -0.75     | -1.21         | -          |
| $\Xi^0$    | -0.06     | -0.10         | -          |
| $\Xi^-$    | -0.72     | -1.21         | -          |

values of the collective operators. In particular, the terms with the  $I_2$  in Eq. (54) can be understood as kaonic contributions in the mesonic language [45]. They are relevant to the hidden strangeness having an effect on the nucleon.

We now turn our attention to the other SU(3) hyperons. In Figs. 6 and 7, we present the electric form factors for the SU(3) octet hyperons. Figure 6 draws those of charged hyperons while Fig. 7 displays those of neutral ones. Without  $m_s$  correction, we could observe  $U$ -spin symmetry expressed by

$$\begin{aligned} G_{E,M}^p &= G_{E,M}^{\Sigma^+}, & G_{E,M}^{\Sigma^-} &= G_{E,M}^{\Xi^-}, \\ G_{E,M}^n &= G_{E,M}^{\Xi^0}, & G_{E,M}^\Lambda &= -G_{E,M}^{\Sigma^0}. \end{aligned} \quad (59)$$

Figures 6 and 7 show us SU(3) symmetry breaking arising from the  $m_s$  correction. In case of the charged octet baryons, the SU(3) splittings of the electric form factors are rather small while they are quite visible for the neutral ones. The predicted electric charge radii for different baryons are listed in Table I, compared with the SU(3) Skyrme model with pseudoscalar vector mesons [37].

#### IV. MAGNETIC PROPERTIES OF THE SU(3) OCTET BARYONS

The space components of the electromagnetic current are responsible for the magnetic form factors. As used in case of the electric form factor, we again make use of the projection operators given in Eq. (52) and SU(2) $_T \times$ U(1) $_Y$ -invariant tensors, so that we obtain the expression of  $G_M^B(\vec{Q}^2)$ :

$$\begin{aligned} G_M^B(\vec{Q}^2) &= \frac{M_N}{|\vec{Q}|} \left[ \langle D_{Q3}^{(8)} \rangle_B \left( \mathcal{Q}_0(\vec{Q}^2) + \frac{\mathcal{Q}_1(\vec{Q}^2)}{I_1} + \frac{\mathcal{Q}_2(\vec{Q}^2)}{I_2} \right) - \langle D_{Q8}^{(8)} J_3 \rangle_B \frac{\mathcal{X}_1(\vec{Q}^2)}{\sqrt{3}I_1} - \langle d_{3pq} D_{Qp}^{(8)} J_q \rangle_B \delta_{pq} \frac{\mathcal{X}_2(\vec{Q}^2)}{I_2} \right. \\ &\quad + 2m_s \langle (D_{88}^{(8)} - 1) D_{Q3}^{(8)} \rangle_B \mathcal{M}_0(\vec{Q}^2) + m_s \langle D_{83}^{(8)} D_{Q8}^{(8)} \rangle_B \left( 2\mathcal{M}_1(\vec{Q}^2) - \frac{2}{3} r_1 \mathcal{X}_1(\vec{Q}^2) \right) \\ &\quad \left. + m_s \sqrt{3} \langle d_{3pq} D_{8p}^{(8)} D_{Qq}^{(8)} \rangle_B \delta_{pq} \left( 2\mathcal{M}_2(\vec{Q}^2) - \frac{2}{3} r_2 \mathcal{X}_2(\vec{Q}^2) \right) \right], \end{aligned} \quad (60)$$

where

$$\mathcal{Q}_0(\vec{Q}^2) = N_c \int d^3x j_1(qr) \left[ \Psi_{\text{val}}^\dagger(x) \gamma_5 \{ \hat{r} \times \vec{\sigma} \} \cdot \vec{\tau} \Psi_{\text{val}}(x) - \frac{1}{2} \sum_n \text{sgn}(E_n) \Psi_n^\dagger(x) \gamma_5 \{ \hat{r} \times \vec{\sigma} \} \cdot \vec{\tau} \Psi_n(x) \mathcal{R}(E_n) \right],$$

$$\begin{aligned} \mathcal{Q}_1(\vec{Q}^2) = & \frac{iN_c}{2} \sum_n \int d^3x j_1(qr) \int d^3y \left[ \text{sgn}(E_n) \frac{\Psi_n^\dagger(x) \gamma_5 \{ \hat{r} \times \vec{\sigma} \} \times \vec{\tau} \Psi_{\text{val}}(x) \cdot \Psi_{\text{val}}^\dagger(y) \vec{\tau} \Psi_n(y)}{E_n - E_{\text{val}}} \right. \\ & \left. + \frac{1}{2} \sum_m \Psi_n^\dagger(x) \gamma_5 \{ \hat{r} \times \vec{\sigma} \} \cdot \vec{\tau} \Psi_m(x) \cdot \Psi_m^\dagger(y) \vec{\tau} \Psi_n(y) \mathcal{R}_Q(E_n, E_m) \right], \end{aligned}$$

$$\begin{aligned} \mathcal{Q}_2(\vec{Q}^2) = & \frac{N_c}{2} \sum_{m^0} \int d^3x j_1(qr) \int d^3y \left[ \text{sgn}(E_{m^0}) \frac{\Psi_{m^0}^\dagger(x) \gamma_5 \{ \hat{r} \times \vec{\sigma} \} \cdot \vec{\tau} \Psi_{\text{val}}(x) \Psi_{\text{val}}^\dagger(y) \Psi_{m^0}(y)}{E_{m^0} - E_{\text{val}}} \right. \\ & \left. + \sum_n \Psi_n^\dagger(x) \gamma_5 \{ \hat{r} \times \vec{\sigma} \} \cdot \vec{\tau} \Psi_{m^0}(x) \Psi_{m^0}^\dagger(y) \Psi_n(y) \mathcal{R}_Q(E_n, E_{m^0}) \right], \end{aligned}$$

$$\begin{aligned} \mathcal{R}_1(\vec{Q}^2) = & N_c \sum_n \int d^3x j_1(qr) \int d^3y \\ & \times \left[ \frac{\Psi_n^\dagger(x) \gamma_5 \{ \hat{r} \times \vec{\sigma} \} \Psi_{\text{val}}(x) \cdot \Psi_{\text{val}}^\dagger(y) \vec{\tau} \Psi_n(y)}{E_n - E_{\text{val}}} + \frac{1}{2} \sum_m \Psi_n^\dagger(x) \gamma_5 \{ \hat{r} \times \vec{\sigma} \} \Psi_m(x) \cdot \Psi_m^\dagger(y) \vec{\tau} \Psi_n(y) \mathcal{R}_M(E_n, E_m) \right], \end{aligned}$$

$$\begin{aligned} \mathcal{R}_2(\vec{Q}^2) = & N_c \sum_{m^0} \int d^3x j_1(qr) \int d^3y \left[ \frac{\Psi_{m^0}^\dagger(x) \gamma_5 \{ \hat{r} \times \vec{\sigma} \} \cdot \vec{\tau} \Psi_{\text{val}}(x) \Psi_{\text{val}}^\dagger(y) \Psi_{m^0}(y)}{E_{m^0} - E_{\text{val}}} \right. \\ & \left. + \sum_n \Psi_n^\dagger(x) \gamma_5 \{ \hat{r} \times \vec{\sigma} \} \cdot \vec{\tau} \Psi_{m^0}(x) \Psi_{m^0}^\dagger(y) \Psi_n(y) \mathcal{R}_M(E_n, E_{m^0}) \right], \end{aligned}$$

$$\begin{aligned} \mathcal{M}_0(\vec{Q}^2) = & \frac{N_c}{3} \sum_n \int d^3x j_1(qr) \int d^3y \left[ \frac{\Psi_n^\dagger(x) \gamma_5 \{ \hat{r} \times \vec{\sigma} \} \cdot \vec{\tau} \Psi_{\text{val}}(x) \Psi_{\text{val}}^\dagger(y) \beta \Psi_n(y)}{E_n - E_{\text{val}}} \right. \\ & \left. + \frac{1}{2} \sum_m \Psi_n^\dagger(x) \gamma_5 \{ \hat{r} \times \vec{\sigma} \} \cdot \vec{\tau} \Psi_m(x) \Psi_m^\dagger(y) \beta \Psi_n(y) \mathcal{R}_\beta(E_n, E_m) \right], \end{aligned}$$

$$\begin{aligned} \mathcal{M}_1(\vec{Q}^2) = & \frac{N_c}{3} \sum_n \int d^3x j_1(qr) \int d^3y \left[ \frac{\Psi_n^\dagger(x) \gamma_5 \{ \hat{r} \times \vec{\sigma} \} \Psi_{\text{val}}(x) \cdot \Psi_{\text{val}}^\dagger(y) \beta \vec{\tau} \Psi_n(y)}{E_n - E_{\text{val}}} \right. \\ & \left. + \frac{1}{2} \sum_m \Psi_n^\dagger(x) \gamma_5 \{ \hat{r} \times \vec{\sigma} \} \Psi_m(x) \cdot \Psi_m^\dagger(y) \beta \vec{\tau} \Psi_n(y) \mathcal{R}_\beta(E_n, E_m) \right], \end{aligned}$$

$$\begin{aligned} \mathcal{M}_2(\vec{Q}^2) = & \frac{N_c}{3} \sum_{m^0} \int d^3x j_1(qr) \int d^3y \left[ \frac{\Psi_{m^0}^\dagger(x) \gamma_5 \{ \hat{r} \times \vec{\sigma} \} \cdot \vec{\tau} \Psi_{\text{val}}(x) \Psi_{\text{val}}^\dagger(y) \beta \Psi_{m^0}(y)}{E_{m^0} - E_{\text{val}}} \right. \\ & \left. + \sum_n \Psi_n^\dagger(x) \gamma_5 \{ \hat{r} \times \vec{\sigma} \} \cdot \vec{\tau} \Psi_{m^0}(x) \Psi_{m^0}^\dagger(y) \beta \Psi_n(y) \mathcal{R}_\beta(E_n, E_{m^0}) \right]. \end{aligned} \tag{61}$$

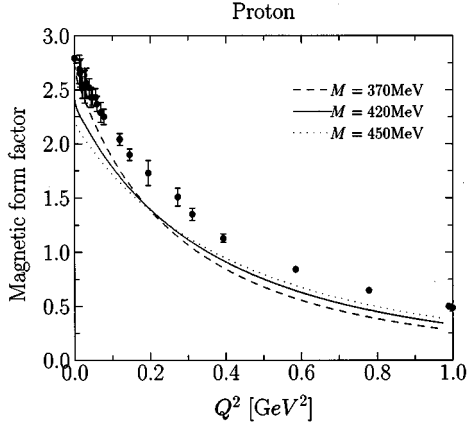


FIG. 8. The proton magnetic form factor as a function of  $Q^2$ : The dashed curve corresponds to the constituent quark mass  $M=370$  MeV, while solid curve is for  $M=420$  MeV. The dotted curve displays the case of  $M=450$  MeV. The empirical data are taken from Höhler *et al.* [38]. The numbers are given in units of the Bohr-magneton without any rescaling.

The regularization functions  $\mathcal{R}$ ,  $\mathcal{R}_Q$ ,  $\mathcal{R}_M$ , and  $\mathcal{R}_\beta$  are defined in Eq. (49). The subscripts  $p$  and  $q$  in Eq. (60) designate flavor indices from 4 to 7. The  $m^0$  in the summation stands for the vacuum states with the SU(2) flavor.  $r_i$  is  $K_i/I_i$  for short. As we can see from the densities for the magnetic form factors in Eq. (61), they are pure SU(2) quantities. The SU(3) components are only found in the collective operators in Eq. (60). Therefore, it is straightforward to calculate Eq. (60) numerically. To make sure, we have compared the density of each contribution with the corresponding density in the gradient expansion given in Appendix B. As the soliton size increases, our expressions converge to those of the gradient expansion.

The nucleon magnetic form factors are displayed in Figs. 8 and 9, as the constituent quark mass is varied from

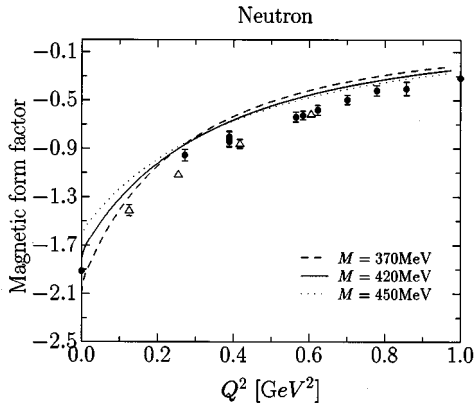


FIG. 9. The neutron magnetic form factor as a function of  $Q^2$ : The dashed curve corresponds to the constituent quark mass  $M=370$  MeV, while solid curve is for  $M=420$  MeV. The dotted curve displays the case of  $M=450$  MeV. The empirical data represented by black dots are taken from Höhler *et al.* [38] while the data with open triangles are from the most recent experiment [47]. The numbers are given in units of the Bohr-magneton without any rescaling.

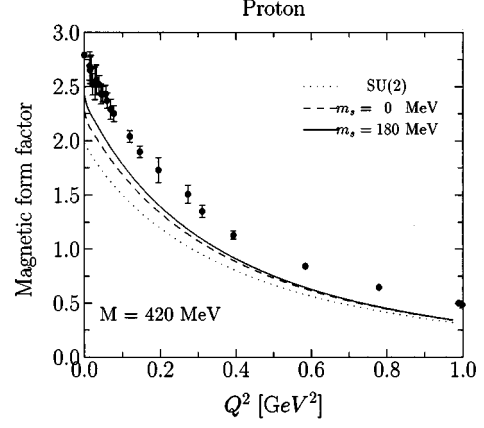


FIG. 10. The proton magnetic form factor as a function of  $Q^2$ : The solid curve corresponds to the strange quark mass  $m_s=180$  MeV, while dashed curve draws without  $m_s$ . The dotted curve displays that of the SU(2) model.  $M=420$  MeV is chosen for the constituent quark mass. The empirical data are taken from Höhler *et al.* [38]. The numbers are given in units of the Bohr-magneton without any rescaling.

$M=370$  MeV to  $M=450$  MeV. In contrast to the case of the electric form factors, the dependence of the magnetic form factors on the constituent quark mass is not linear. Up to around  $Q^2=0.2$  GeV<sup>2</sup> in case of the proton ( $Q^2=0.4$  GeV<sup>2</sup> for the neutron), smaller constituent quark masses are more contributive to the magnetic form factors. However, as  $Q^2$  increases, the dependence on the constituent quark mass undergoes a change, i.e., the greater constituent quark masses contribute more to the magnetic form factors. In fact, we can reach the empirical data in the vicinity of  $Q^2=0$  with  $M=370$  MeV, we reproduce roughly the correct momentum dependence. We select  $M=420$  MeV for the best fit to be consistent with all observables in this paper.

Figures 10 and 11 present the contributions of the strange

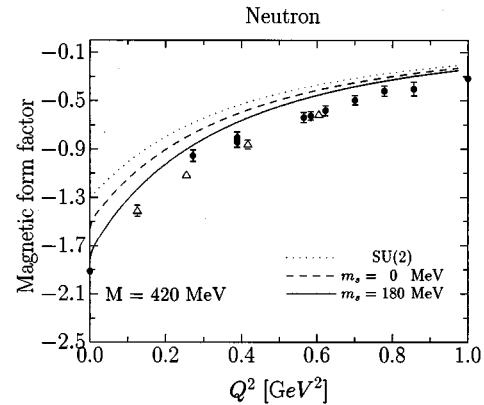


FIG. 11. The neutron magnetic form factor as a function of  $Q^2$ : The solid curve corresponds to the strange quark mass  $m_s=180$  MeV, while dashed curve draws without  $m_s$ . The dotted curve displays the case of the SU(2) model.  $M=420$  MeV is chosen for the constituent quark mass. The empirical data represented by black dots are taken from Höhler *et al.* [38] while the data with open triangles are from the most recent experiment [47]. The numbers are given in units of the Bohr-magneton without any rescaling.

TABLE II. The magnetic moments of the SU(3) octet baryons predicted by our model. Each contribution is listed from the leading order. The results are also compared with the Skyrme model of Park and Weigel [37]. The experimental data for the magnetic moments are taken from Ref. [45]. Our final values are given by  $\mu_B(\Omega^1, m_s^1)$ . The constituent quark mass is fixed to  $M = 420$  MeV.

| Baryons                          | $\mu_B(\Omega^0, m_s^0)$ | $\mu_B(\Omega^1, m_s^0)$ | $\mu_B(\Omega^1, m_s^1)$ | Park & Weigel | Expt. |
|----------------------------------|--------------------------|--------------------------|--------------------------|---------------|-------|
| $p$                              | 1.01                     | 2.27                     | 2.39                     | 2.36          | 2.79  |
| $n$                              | -0.75                    | -1.55                    | -1.76                    | -1.87         | -1.91 |
| $\Lambda$                        | -0.38                    | -0.78                    | -0.77                    | -0.60         | -0.61 |
| $\Sigma^+$                       | 1.01                     | 2.27                     | 2.42                     | 2.41          | 2.46  |
| $\Sigma^0$                       | 0.38                     | 0.78                     | 0.75                     | 0.66          | -     |
| $\Sigma^-$                       | -0.25                    | -0.71                    | -0.92                    | -1.10         | -1.16 |
| $\Xi^0$                          | -0.75                    | -1.55                    | -1.64                    | -1.96         | -1.25 |
| $\Xi^-$                          | -0.25                    | -0.71                    | -0.68                    | -0.84         | -0.65 |
| $ \Sigma^0 \rightarrow \Lambda $ | 0.65                     | 1.34                     | 1.51                     | 1.74          | 1.61  |

quark mass. On the contrary to the electric form factors, the  $m_s$  correction enhances the magnetic form factors about 5% to 10%. In particular, it is of great significance for the neutron magnetic form factor in fitting the empirical data as shown in Fig. 11. Our theoretical magnetic form factors are in good agreements with the empirical data within about 15% as the other quantities.

Table II shows each contribution of the rotational  $1/N_c$  and  $m_s$  corrections to the magnetic moments, i.e.,  $G_M^B(Q^2)$  at  $Q^2=0$  (in Ref. [28], the magnetic moments are discussed in detail). Our results are compared with the SU(3) Skyrme model with pseudoscalar vector meson [37]. Figures 12 and 13 display the magnetic form factors of the charged and neutral octet baryons, respectively. The explicit breaking of  $U$ -spin symmetry in the magnetic form factors are observed. The corresponding magnetic charge radii are defined by

$$\langle r^2 \rangle_M^B = - \frac{6}{\mu_B} \frac{dG_M^B(Q^2)}{dQ^2} \Big|_{Q^2=0}. \quad (62)$$

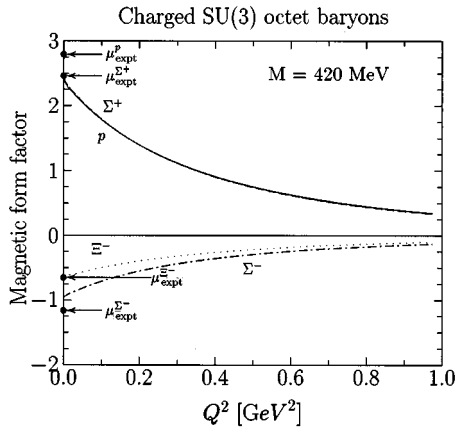


FIG. 12. The magnetic form factors of the charged SU(3) octet baryons as a function of  $Q^2$ : The solid curve corresponds to the proton magnetic form factor. The dashed curve is for  $\Sigma^+$ . The dash-dotted curve displays that of  $\Sigma^-$  and the dotted curve that of  $\Xi^-$ . The experimental data for the magnetic moments are taken from Ref [46].  $M = 420$  MeV is chosen for the constituent quark mass.

The numerical results are listed in Table III. The results for the nucleon are in good agreements with the experimental data.

## V. SUMMARY AND CONCLUSION

The aim of this work has been to investigate the electromagnetic form factors of the SU(3) octet baryons and related quantities such as electromagnetic charge radii and magnetic moments in the SU(3) semibosonized NJL model. Starting from the effective chiral action, we have expressed the matrix elements of electromagnetic current in the model. When quantizing the soliton, the contributions arising from the noncommutativity of collective operators were considered. It gives a nonzero contribution of the rotational  $1/N_c$  corrections. The  $m_s$  corrections are treated perturbatively, the collective wave function correction being taken heed of. The octet states of the baryon are mixed with higher irreducible representations because of  $m_s$ .

The parameters of the model, including the cutoff, are adjusted to  $m_\pi = 139$  MeV and  $f_\pi = 93$  MeV. The only pa-

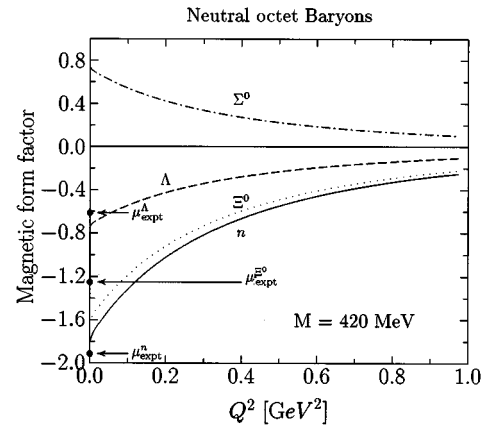


FIG. 13. The magnetic form factors of the neutral SU(3) octet baryons as a function of  $Q^2$ : The solid curve corresponds to the neutron magnetic form factor. The dashed curve is for  $\Lambda$ . The dash-dotted curve displays that of  $\Sigma^0$  and the dotted curve that of  $\Xi^0$ . The experimental data for the magnetic moments are taken from Ref. [46].  $M = 420$  MeV is chosen for the constituent quark mass.

TABLE III. The magnetic charge radii of the SU(3) octet baryons predicted by our model compared with the Skyrme model of Park and Weigel [37]. The constituent quark mass is fixed to  $M = 420$  MeV.

| Baryons    | Our model | Park & Weigel | Experiment |
|------------|-----------|---------------|------------|
| $p$        | 0.70      | 0.94          | 0.74       |
| $n$        | 0.78      | 0.94          | 0.77       |
| $\Lambda$  | 0.70      | 0.78          | –          |
| $\Sigma^+$ | 0.71      | 0.96          | –          |
| $\Sigma^0$ | 0.70      | 0.86          | –          |
| $\Sigma^-$ | 0.74      | 1.07          | –          |
| $\Xi^0$    | 0.75      | 0.90          | –          |
| $\Xi^-$    | 0.51      | 0.84          | –          |

parameter we have in the model is the constituent quark mass  $M$  which is fixed to  $M = 420$  MeV by the mass splitting of the SU(3) baryons. The electric form factor of the proton is in an excellent agreement with the empirical data. As far as the electric form factor of the neutron is concerned, it is well known that there are large uncertainties in extracting it from experiments [42]. However, compared to Ref. [43], our result is found to be in a remarkable agreement with it. The electric charge radii of the nucleon are also obtained in good agreement with the experimental result within about 10%.

We also evaluated electric and magnetic form factors of all other members of the SU(3) baryon octet. The magnetic moments are in a good agreement with the experimental data. As far as the  $Q^2$  dependence is concerned, since there are no experimental data available, these numbers are predictions. In all cases, the  $m_s$  corrections are about 10%.

Electromagnetic form factors of the baryons are used in order to extract strange form factors from the experimental data. The evaluation of these quantities and of semileptonic and mesonic decays of hyperons will be the next steps in our research.

#### ACKNOWLEDGMENTS

We would like to thank Ch. Christov, P. Pobylitsa, M. Praszalowicz, and T. Watabe for fruitful discussions and critical comments. This work has partly been supported by the BMFT, the DFG, and the COSY Project (Jülich). The work of M.P. was supported in part by Grant No. INTAS-93-0283.

#### APPENDIX A: THE DERIVATION OF THE REGULARIZATION

In this appendix, we shall give an explicit derivation of the regularized  $\Omega^0$  and  $\Omega^1$  contributions to the electromagnetic form factors. We make use of the proper-time regularization scheme. We can see that the procedure is very similar to the case of the axial constants [20]. Note that the non-anomalous part is regularized. As is written in Eq. (44), the regularized effective action is expressed as

$$\text{Re}S_{\text{eff}} = \text{Sp} \int \frac{du}{u} \phi(u; \Lambda_i) \exp(-uDD^\dagger), \quad (\text{A1})$$

where

$$D = \partial_\tau + H + i\Omega_E + \beta A^\dagger \hat{Q}A - iA_4 A^\dagger \hat{Q}A - \alpha_k A_k A^\dagger \hat{Q}A, \\ D^\dagger = -\partial_\tau + H - i\Omega_E + \beta A^\dagger \hat{Q}A + iA_4 A^\dagger \hat{Q}A - \alpha_k A_k A^\dagger \hat{Q}A, \quad (\text{A2})$$

Hence,

$$DD^\dagger = W_0(A_\mu^0, \Omega^0, m^0) + W_1(A_\mu^1, \Omega^0, m^0) + W_2(A_\mu^1, \Omega^1) \\ + W_3(A_\mu^0, \Omega^1) + W_4(m^1) + O(\Omega^1, m^1) + O(\Omega^2) \\ + O(m^2), \quad (\text{A3})$$

with

$$W_0 = -\partial_\tau^2 + H_E^2,$$

$$W_1 = i\{A_4 A^\dagger \hat{Q}A, \partial_\tau\} - [\alpha_k A_k A^\dagger \hat{Q}A, \partial_\tau] - i[H_E, A_4 A^\dagger \hat{Q}A] \\ - \{H_E, \alpha_k A_k A^\dagger \hat{Q}A\},$$

$$W_2 = -\{\Omega_E, A_4 A^\dagger \hat{Q}A\} + i[\Omega_E, \alpha_k A_k A^\dagger \hat{Q}A],$$

$$W_3 = -i\{\Omega_E, \partial_\tau\} + i[H_E, \Omega_E],$$

$$W_4 = [\beta A^\dagger \hat{m}A, \partial_\tau] + \{H_E, \beta A^\dagger \hat{m}A\} - i[\beta A^\dagger \hat{m}A, A_4 A^\dagger \hat{Q}A] \\ + \{\beta A^\dagger \hat{m}A, \alpha_k A_k A^\dagger \hat{Q}A\}. \quad (\text{A4})$$

The terms of higher orders in  $\Omega$  and  $\hat{m}$  and of  $\Omega \cdot \hat{m}$  are neglected, since they are believed to be very tiny.

Taking advantage of the Feynman-Schwinger-Dyson formula, we can expand  $\exp(-uW)$  around  $W_0$ :

$$\exp(-uW) = \exp(-uW_0) - u \int_0^1 d\alpha \exp(-u\alpha W_0) \\ \times [W - W_0] \exp(-u(1-\alpha)W_0) \\ + u^2 \int_0^1 d\beta \int_0^{1-\beta} \exp(-u\alpha W_0) [W - W_0] \\ \times \exp(-u\beta W_0) [W - W_0] \\ \times \exp[-u(1-\alpha-\beta)W_0] + \dots \quad (\text{A5})$$

First, we shall consider in case of the electric form factor. The lowest order contribution of  $\Omega_E$  vanishes. The sea contribution of  $\Omega_E^0$  comes only from the imaginary part of the effective action. As for the next order of  $\Omega_E$ , we need  $W_2$  and  $W_1 \cdot W_3$ . After some manipulations, we obtain

$$\langle B, p' | V_0(0) | B, p \rangle^{\Omega^1} = \frac{N_c}{4} \sum_{nm} R_I(E_n, E_m) \langle \{D_{Qa}^{(8)}, i\Omega_E^b\} \rangle_B \\ \times \int d^3x e^{i\vec{q} \cdot \vec{x}} \\ \times \int d^3y \Psi_n^\dagger(x) \lambda^a \Psi_m(x) \\ \times \Psi_m^\dagger(y) \lambda^b \Psi_n(y). \quad (\text{A6})$$

The  $m_s$  correction because of  $W_4$  and  $W_4 \cdot W_1$  vanishes as the  $\Omega^0$  contribution. The  $m_s$  correction arises only from the quantization of  $i\Omega_E$  [23].

The regularization of the magnetic form factor is more involved because of the time ordering of collective operators. Here, we need only the term  $-A_k\{H_E, \alpha_k A^\dagger \hat{Q}A\}$  for the lowest order contribution:

$$\begin{aligned} & \langle B, p' | V_i(0) | B, p \rangle^{\Omega^0} \\ &= \frac{1}{2} \frac{\delta}{\delta A_i} \text{Sp} \int du \phi(u; \Lambda_i) \int_0^1 d\alpha \\ & \quad \times \exp(-u\alpha W_0) A_k \{H_E, \alpha_k A^\dagger \hat{Q}A\} \exp[-u(1-\alpha)W_0] \\ &= \frac{N_c}{2} D_{Qa}^{(8)} \sum_n \langle n | \alpha_i \lambda^a | n \rangle R(E_n), \end{aligned} \quad (\text{A7})$$

where  $R(E_n)$  is defined in Eq. (49).

As a next step, we proceed to evaluate the  $\Omega_E^1$  correction to the magnetic form factor. It is tedious but straightforward:

$$\langle B, p' | V_i(0) | B, p \rangle^{\Omega^1} = \frac{\delta}{\delta A_i} (X_1[A_k] + X_2[A_k])_{A_k=0}, \quad (\text{A8})$$

where

$$\begin{aligned} X_1[A_k] &= \frac{1}{2} \text{Sp} \int du \phi(u; \Lambda_i) \int_0^1 d\alpha \exp(-u\alpha W_0) W_2[A_k] \\ & \quad \times \exp[-u(1-\alpha)W_0], \end{aligned} \quad (\text{A9})$$

$$\begin{aligned} X_2[A_k] &= \frac{1}{2} \text{Sp} \int du \phi(u; \Lambda_i) \int_0^1 d\beta \int_0^{1-\beta} d\alpha \exp(-u\alpha W_0) \\ & \quad \times (W_1[A_k] + W_3[A_k]) \exp(-u\beta W_0) \\ & \quad \times (W_1[A_k] + W_3[A_k]) \exp[-u(1-\alpha-\beta)W_0]. \end{aligned} \quad (\text{A10})$$

The terms including  $W_1 \cdot W_1$  and  $W_3 \cdot W_3$  vanish. The first term  $\delta/\delta A_i X_1[A_k]$  is obtained to be

$$\begin{aligned} \frac{\delta}{\delta A_i} X_1[A_k] &= \frac{-i}{16} N_c \sum_{n,m} \sqrt{\frac{u}{\pi}} (e^{-uE_n^2} - e^{-uE_m^2}) \{i\Omega_E^a, D_{Qb}^{(8)}\} \\ & \quad \times \langle n | \lambda^a | m \rangle \langle m | \alpha_i \lambda^b | m \rangle. \end{aligned} \quad (\text{A11})$$

The second term is

$$\begin{aligned} \frac{\delta}{\delta A_i} X_2[A_k] &= -u \frac{iN_c}{8\pi} \sum_{n,m} \int_0^1 d\beta e^{-u[\beta E_m^2 + (1-\beta)E_n^2]} \\ & \quad \times [\beta E_m - (1-\beta)E_n] \frac{1}{\sqrt{\beta(1-\beta)}} [i\Omega_E^a, D_{Qb}] \\ & \quad \times \langle n | \lambda^a | m \rangle \langle m | \alpha_i \lambda^b | n \rangle \\ & \quad + \frac{i}{16} N_c \sum_{n,m} \sqrt{\frac{u}{\pi}} (e^{-uE_n^2} - e^{-uE_m^2}) \{i\Omega_E^a, D_{Qb}^{(8)}\} \\ & \quad \times \langle n | \lambda^a | m \rangle \langle m | \alpha_i \lambda^b | n \rangle. \end{aligned} \quad (\text{A12})$$

The second part of Eq. (A12) is canceled by  $\delta/\delta A_i X_1[A_k]$ , so that we have

$$\begin{aligned} & \langle B, p' | V_i(0) | B, p \rangle^{\Omega^1} \\ &= -u \frac{iN_c}{8\pi} \sum_{n,m} \int_0^1 d\beta e^{-u[\beta E_m^2 + (1-\beta)E_n^2]} \\ & \quad \times [\beta E_m - (1-\beta)E_n] \frac{1}{\sqrt{\beta(1-\beta)}} [i\Omega_E^a, D_{Qb}] \\ & \quad \times \langle n | \lambda^a | m \rangle \langle m | \alpha_i \lambda^b | n \rangle. \end{aligned} \quad (\text{A13})$$

Having integrated over  $\beta$ , we obtain

$$\begin{aligned} \langle B, p' | V_i(0) | B, p \rangle^{\Omega^1} &= -\frac{N_c}{4} \sum_m \langle [D_{Qa}^{(8)}, J_b] \rangle_B \langle n | \lambda^a | m \rangle \\ & \quad \times \langle m | \alpha_i \lambda^b | n \rangle \mathcal{R}_Q(E_n, E_m), \end{aligned} \quad (\text{A14})$$

where  $\mathcal{R}_Q$  is defined in Eq. (49).

## APPENDIX B: THE GRADIENT EXPANSION OF THE MAGNETIC MOMENTS

It is well known that the exact expressions for the magnetic moments can be expanded in powers of gradients of the chiral fields [48]. In this way the quark determinant gives terms, which are quite similar to the Skyrme model expressions [37]. An important difference is, however, the contributions of order  $\Omega^1$  from the real part of the action. In the present case we obtain

$$\begin{aligned} \mu_B &= -2M_n \int dr r^2 \sin^2 \theta \langle D_{Q3} \rangle_B \left[ \frac{8\pi}{3} f_\pi^2 + \frac{1}{3} \frac{M_u}{4I_1} + \frac{1}{3} \frac{M_u}{8I_2} \right] \\ & \quad + \frac{4}{9\pi} \int dr r^2 \sin^2 \theta \theta' \left[ \frac{-\langle d_{3pp} D_{Qp} J_p \rangle_B}{I_2} - \frac{\langle D_{Q8} J_3 \rangle_B}{I_1 \sqrt{3}} \right]. \end{aligned} \quad (\text{B1})$$

Our numerical densities for the electromagnetic form factors are compared with those obtained from the gradient expansion in order to warrant the calculation.



- [1] S. Kahana, G. Ripka, and V. Soni, Nucl. Phys. **A415**, 351 (1984).
- [2] M.S. Birse and M.K. Banerjee, Phys. Lett. **136B** (1984).
- [3] V. Soni, Phys. Lett. B **183**, 91 (1987).
- [4] D. Diakonov and V. Petrov, Nucl. Phys. **B272**, 457 (1986).
- [5] D. Diakonov, V. Petrov, and P. Pobylitsa, Nucl. Phys. **B272**, 809 (1988).
- [6] H. Reinhardt and R. Wunsch, Phys. Lett. B **215**, 577 (1988).
- [7] Th. Meissner, F. Grümmer, and K. Goeke, Phys. Lett. B **227**, 296 (1989).
- [8] M. Wakamatsu and H. Yoshiki, Nucl. Phys. **A524**, 561 (1991).
- [9] G.S. Adkins, C.R. Nappi, and E. Witten, Nucl. Phys. **B228**, 552 (1983).
- [10] P. Ring and P. Schuck, *The Nuclear Many-Body Problem* (Springer-Verlag, New York, 1980).
- [11] K. Goeke, A.Z. Górski, F. Grümmer, Th. Meissner, H. Reinhardt, and R. Wunsch, Phys. Lett. B **256**, 321 (1991).
- [12] M. Wakamatsu and T. Watabe, Phys. Lett. B **312**, 184 (1993).
- [13] C.V. Christov, A. Blotz, K. Goeke, P. Pobylitsa, V. Petrov, M. Wakamatsu, and T. Watabe, Phys. Lett. B **325**, 467 (1994).
- [14] M. Wakamatsu, Phys. Rev. D **46**, 3762 (1992).
- [15] Ch. Christov, A.Z. Górski, K. Goeke, and P.V. Pobylitsa, RUB-TPII-2/94, Nucl. Phys. A (to be published).
- [16] A. Blotz, Ph.D. thesis, Ruhr-Universität Bochum, 1994.
- [17] H.-C. Kim, A. Blotz, C. Schneider, and K. Goeke, Nucl. Phys. A (to be published).
- [18] A. Blotz, M. Praszalowicz, and K. Goeke, Acta Phys. Polon. B **35**, 1443 (1994).
- [19] H.-C. Kim, T. Watabe, and K. Goeke, Report No. RUB-TPII-11/95 [hep-ph/9506344], 1995 (unpublished).
- [20] A. Blotz, M. Praszalowicz, and K. Goeke, Phys. Lett. B **317**, 195 (1994).
- [21] A. Blotz, M. Praszalowicz, and K. Goeke, Phys. Rev. D **53**, 485 (1996).
- [22] A. Blotz, D. Diakonov, K. Goeke, N.W. Park, V. Petrov, and P.V. Pobylitsa, Phys. Lett. B **287**, 29 (1992).
- [23] A. Blotz, D. Diakonov, K. Goeke, N.W. Park, V. Petrov, and P.V. Pobylitsa, Nucl. Phys. **A555**, 765 (1993).
- [24] H. Weigel, R. Alkofer, and H. Reinhardt, Nucl. Phys. **B387**, 638 (1992).
- [25] A. Blotz, M.V. Polyakov, and K. Goeke, Phys. Lett. B **302**, 151 (1993).
- [26] A. Blotz, M. Praszalowicz, and K. Goeke, Phys. Lett. B **317**, 195 (1993).
- [27] M. Praszalowicz, A. Blotz, and K. Goeke, Phys. Rev. D **47**, 1127 (1993).
- [28] H.-C. Kim, M. Polyakov, A. Blotz, and K. Goeke, Nucl. Phys. A (to be published).
- [29] R. Ball, Phys. Rep. **182**, 1 (1989).
- [30] C. Itzykson and J.-B. Zuber, *Quantum Field Theory* (McGraw-Hill, New York, 1980).
- [31] E. Guadagnini, Nucl. Phys. **B236**, 35 (1984).
- [32] N. Toyota, Prog. Theor. Phys. **77**, 688 (1987).
- [33] J.J. de Swart, Rev. Mod. Phys. **35**, 916 (1963).
- [34] P. McNamee, S.J. and F. Chilton, Rev. Mod. Phys. **36**, 1005 (1964).
- [35] P. Pobylitsa (private communication).
- [36] S. Kahana and G. Ripka, Nucl. Phys. **A429**, 462 (1984).
- [37] N.W. Park and H. Weigel, Nucl. Phys. **A541**, 453 (1992).
- [38] G. Höhler *et al.*, Nucl. Phys. **B114**, 505 (1976).
- [39] S. Platchkov *et al.*, Nucl. Phys. **A510**, 740 (1990).
- [40] C.E. Jones-Woodward *et al.*, Phys. Rev. C **44**, R571 (1991).
- [41] A.K. Thompson *et al.*, Phys. Rev. Lett. **68**, 2901 (1992).
- [42] T. Eden *et al.*, Phys. Rev. C **50**, R1749 (1994).
- [43] M. Meyerhoff *et al.*, Phys. Lett. B **327**, 201 (1994).
- [44] S. Kopecky, P. Riehs, J.A. Harvey, and N.W. Hill, Phys. Rev. Lett. **74**, 2427 (1995).
- [45] T. Watabe, H.-C. Kim, and K. Goeke, Report No. RUB-TPII-17/95, [hep-ph/9507318], 1995 (unpublished).
- [46] Particle Data Group, L. Montanet *et al.*, Phys. Rev. D **50**, 1173 (1994), p. 1218.
- [47] E.E.W. Bruins *et al.*, Phys. Rev. Lett. **75**, 21 (1995).
- [48] J.R. Aitchison and C. Frazer, Phys. Rev. D **31**, 2608 (1985).